

## Article

# Peak Ground Acceleration Mapping of Indonesia Using Complementary Area Source and Smoothed Seismicity Approaches

### Article Info

#### Article history :

Received April 28, 2026

Revised Mei 05, 2026

Accepted Mei 11, 2026

Published June 30, 2026

#### Keywords :

Earthquake source,  
smoothing seismicity,  
probabilistic seismic hazard  
analysis,  
peak ground acceleration

Eka Nioisa Br Surbakti<sup>1</sup>, Ardian Saputra<sup>1</sup>, Rizki Wulandari<sup>1,2\*</sup>,  
Yudha Styawan<sup>1,2</sup>

<sup>1</sup>Department of Geophysical Engineering, Faculty of Industrial Technology, Institut Teknologi Sumatera, Lampung, Indonesia

<sup>2</sup>Center for Earthquake and Tsunami Disaster Mitigation, Institut Teknologi Sumatera, Lampung, Indonesia

**Abstract.** Seismic hazard assessment in tectonically complex regions requires reliable earthquake source modeling to support risk mitigation and building code development. In Indonesia, the choice between area source and smoothed seismicity approaches has been driven by data availability rather than scientific evaluation, and no systematic comparison of both methods at the national scale has been conducted. This study compared both approaches across Indonesia to evaluate their differences in PGA estimation and assess the forecasting skill of the smoothed seismicity model. Both models were applied to the same declustered earthquake catalog using identical Ground Motion Prediction Equations within a probabilistic seismic hazard analysis framework. Both models consistently identified North Sulawesi as the highest hazard region and Kalimantan as the lowest. The smoothed seismicity model produced higher maximum PGA values of 2.13 g compared to 1.1597 g and 1.5901 g from the area source model at 10% and 2% probability of exceedance in 50 years, respectively. Molchan Diagram validation for smoothing seismicity yielded an Area Skill Score of 0.88 and R-score of 0.656, confirming strong forecasting skill. The two methods are complementary, and their integration within a logic tree framework is recommended for future national-scale PSHA in Indonesia.

*This is an open access article under the [CC-BY](https://creativecommons.org/licenses/by/4.0/) license.*



This is an open access article distributed under the Creative Commons 4.0 Attribution License, which permits unrestricted use, distribution, and reproduction in any medium, provided the original work is properly cited. ©2026 by author.

#### Corresponding Author :

Rizki Wulandari

Department of Geophysical Engineering, Faculty of Industrial Technology,  
Institut Teknologi Sumatera, Lampung, Indonesia

Email : [rizki.wulandari@tg.itera.ac.id](mailto:rizki.wulandari@tg.itera.ac.id)

## 1. Introduction

Indonesia's tectonic setting presents one of the world's highest earthquake hazards. The country sits at the intersection of the Indo-Australian, Eurasian, and Pacific plates. Microplates such as the Philippine and Caroline plates further complicate this system. This configuration generates frequent, large-magnitude earthquakes that threaten communities and infrastructure [1].

To quantify earthquake hazard systematically, Probabilistic Seismic Hazard Analysis (PSHA) has emerged as the standard framework [2]. PSHA estimates the probability that ground shaking will exceed specified thresholds over a given time period [3]. This approach incorporates uncertainties in earthquake magnitude, source location, and recurrence rates. The primary output is Peak Ground Acceleration (PGA), a key parameter for designing earthquake-resistant structures and disaster risk mitigation [4].

Area source models define zones with relatively homogeneous seismicity characteristics. These are used when active faults cannot be clearly identified due to limited geological data or scattered seismicity [5]. Zoning is determined from tectonic, neotectonic, and geological information. This approach has proven effective in the Sumatra region [5] and West Sumatra [6] where multiple source zones distinguish between subduction zones, active faults, and background seismicity. However, area source models rely on subjective zone delineation, which may introduce spatial bias and may not capture complex seismicity patterns in high-uncertainty regions.

Seismicity smoothing offers an alternative to subjective zoning. This data-driven method uses historical earthquake distributions to map spatial patterns [7]. A previous study by Ardian Saputra applied seismicity smoothing to analyze spatial earthquake patterns in Indonesia; however, the study was limited to the smoothing process itself and did not extend to the estimation of PGA values across the entire Indonesian territory [8]. A kernel function distributes earthquake activity continuously across the study area rather than concentrating it at discrete points. This reduces spatial bias from major earthquakes and produces more objective representations of seismicity. Studies applying this method including regional applications in Kalimantan [9] and validations in Bangladesh [10] demonstrate its effectiveness in areas where active fault data are limited. Furthermore, Wulandari and Styawan [11] demonstrated that Gaussian smoothing with a 50 km bandwidth provides the most stable and reliable seismic hazard model for the Lampung region, Sumatra, as validated through the Molchan diagram and Area Skill Score (ASS), confirming its effectiveness in capturing localized seismicity patterns. However, smoothing methods are inherently dependent on the completeness of historical earthquake catalogs. In regions with uneven catalog completeness, this dependence may introduce systematic bias into hazard estimates [7].

Despite these advancements, no study has systematically compared both approaches at a national scale in Indonesia. While existing studies have made valuable contributions using either approach, few have systematically examined how results vary between the two methods and the factors that may account for such differences. This prevents practitioners from making informed methodological choices. The forecasting skill of both methods also remains unvalidated for Indonesia. Assessed area source and smoothed seismicity models in Taiwan using the Molchan Diagram [12], but no equivalent validation exists for the Indonesian context. Moreover, method selection is often driven by data availability rather than scientific rationale. Indonesia's tectonic complexity spanning active subduction zones and diffuse intraplate seismicity likely demands different modeling strategies across regions.

This study addresses these gaps by applying both area source and smoothed seismicity approaches across Indonesia to estimate Peak Ground Acceleration (PGA) values through PSHA. Both methods are applied to the same earthquake catalog covering the entire Indonesian region. The smoothed seismicity model is further validated using the Molchan Diagram to assess its forecasting skill. Our findings will examine whether area source and smoothed seismicity produce different hazard estimates, and whether the two methods can complement each other in estimating PGA values across different tectonic regions of Indonesia. The results are expected to provide a scientific basis for future PSHA implementations and earthquake risk mitigation efforts in Indonesia.

## 2. Research Methodology

### 2.1. Research Location

Earthquake data was obtained from the International Seismological Centre (ISC), a nonprofit organization that compiles global seismological data with open access. The data covers the territory of Indonesia ( $8.5^{\circ}$  N –  $19^{\circ}$  S,  $91^{\circ}$  –  $151^{\circ}$  E) for the period January 1, 1900 – October 2, 2025, with magnitudes ranging from 0 to 10 and depths ranging from 0 to 300 km.

### 2.2. Theoretical Research

Earthquake catalog harmonization was first performed to standardize magnitude scales from various sources (Ms, Mb, Mw, etc.) into a single unified scale. Moment magnitude (Mw) was adopted as the reference scale for all magnitude conversions, as this scale does not experience saturation and explicitly accounts for fault rupture area and displacement [13]. The harmonization procedure followed established methodologies validated for Indonesian earthquake catalogs, utilizing standardized conversion equations to ensure consistency across the entire dataset.

Following harmonization, declustering was applied to isolate mainshocks from foreshocks and aftershocks, retaining only independent seismic events. The Reasenber method was selected for this purpose owing to its ability to objectively characterize spatio-temporal relationships between earthquakes based on distance and time criteria [14]. This method employs adaptive space-time windows to identify clusters of related events, providing superior discrimination compared to fixed-window approaches. This method is particularly well-suited for the Indonesian context, where seismic activity is intense and tectonic complexity varies considerably across subduction zones, active fault systems, and background seismicity zones [15].

Earthquake source modeling was subsequently carried out within the PSHA framework. The analysis was restricted to shallow seismic events occurring at depths of less than 50.1 km, as shallow earthquakes produce significantly higher PGA values due to minimal wave attenuation compared to deeper seismic sources [16]. The key input parameters used in this study are summarized in Table 1, which compares the parameters between the area source and smoothed seismicity modeling approaches.

**Table 1.** Comparison of input parameters used in area source and smoothing seismicity models

Parameter	Area Source	Smoothing Seismicity
Magnitude of Completeness (Mc)	4.7	4.4
Bandwidth	-	100
Depth Filter	<50.1 km	<50.1 km
Minimum Magnitude (Mmin)	4.7	4.4
Maximum Magnitude (Mmax)	6.5	6.5
Time Window	50 years	50 years

Two complementary modeling approaches were employed: the area source model and the seismicity smoothed model. In the area source approach, source zones were delineated based on the tectonic, neotectonic, and geological characteristics of the Indonesian region [5], resulting in 21 shallow earthquake source zones as presented in Table 2. Each source zone is characterized by relatively homogeneous seismicity characteristics and defined tectonic mechanisms (strike-slip, thrust, subduction, or combinations thereof) appropriate to the regional tectonics.

**Table 2.** Segment of 21 Source Areas

No	Zone Name	Mechanisms in the Zone
1	Andaman	Subduction + strike-slip
2	Indo-Australian Plate	Convergent
3	Sumatra Fault	Right-lateral strike-slip
4	Sumatra Transition Zone	Transition zone without faults
5	Sumatra-Kalimantan Transition Zone	Transition zone without faults
6	Indo-Australian Plate	Convergent
7	Java Back Arc	Thrust fault & folds
8	RMKS Fault Transition Zone	Strike-slip
9	Kalimantan Fault	Strike-slip (weak-local)
10	Indo-Australian Plate	Convergent with the presence of a thrust fault
11	Banda Arc, Flores Back Arc	Thrust fault
12	Makassar Strait Thrust	Thrust fault
13	Northern Sulawesi Subduction, Palu-Koro Fault	Right-lateral strike-slip
14	Gorontalo Fault	Strike-slip
15	Seram Strike-Slip	Strike-slip
16	Philippine Megathrust	Subduction
17	Kolaka Fault	Strike-slip
18	Aru Trench, Seram Strike-Slip	Strike-slip
19	Australia-Pacific Convergent Zone Subduction	Subduction + plate collision, Strike-slip
20	Cendrawasih Thrust and Memberamo	Thrust fault
21	Papua FTB	Thrust fault/Reverse

The assessment of seismic catalog completeness and seismicity parameters was performed through the analysis of the magnitude of completeness ( $M_c$ ) and the estimation of a-value and b-value based on the Gutenberg–Richter relationship.  $M_c$  represents the minimum magnitude above which earthquake data are considered complete, and its accurate determination is essential to avoid bias in parameter estimation [17]. The b-value reflects the relative proportion of small to large earthquakes, while the a-value represents the overall level of seismic activity [18].

$$\log_{10} \lambda m = a - bm \quad (1)$$

In Equation (1),  $\lambda m$  denotes the number of earthquakes of a given magnitude,  $a$  represents the level of seismic activity in a region,  $b$  describes the seismotectonic characteristics related to the distribution of earthquake magnitudes, and  $m$  is the earthquake magnitude. The maximum likelihood method is used to determine the values of  $a$  and  $b$ , as shown in Equations (2) and (3).

$$b = \frac{1}{\bar{M} - M_{min}} \log e \quad (2)$$

$$a = \log N (M \geq M_0) + \log(b \ln 10) + M_0 b \quad (3)$$

This study employs the maximum likelihood method because it provides more accurate statistical estimates, reduces bias caused by data gaps in the magnitude interval, and yields reliable values [19]. The calculation of the b-value using the maximum likelihood method follows the formulation proposed by [20] where  $\bar{M}$  is the average magnitude,  $M_{min}$  is the minimum magnitude, and  $e$  is the natural logarithm of Euler's number  $e \approx 2.718$ . For the declustered Indonesian catalog (1900-2025, depths <50.1 km), the maximum likelihood analysis yielded: Magnitude of Completeness

(Mc) = 4.7, a-value = 8.753, and b-value = 0.89. The b-value of 0.89 (less than 1.0) indicates that moderate to large magnitude earthquakes are relatively dominant in Indonesia's seismicity distribution, reflecting high tectonic stress accumulation and the potential for significant earthquake generation consistent with subduction zone environments.

The smoothed seismicity method was subsequently applied as a complementary approach to the area source model, serving both as an independent hazard estimation tool and as a means of validating the spatial distribution of PGA values obtained from the area source analysis. This method models the spatial distribution of seismicity based on historical earthquake data, aiming to reduce uncertainty in the characterization of earthquake sources, particularly in regions where geological data are limited or where active faults have not been clearly identified and mapped [21].

The underlying premise of this approach is that the spatial patterns of past earthquake occurrences serve as statistically meaningful indicators of the potential locations of future seismic events, thereby enabling a data-driven estimation of seismic hazard that does not rely on subjective zone boundary definitions [10]. Spatial smoothing was performed using the Gaussian kernel function [22], which distributes the seismicity rate of each recorded earthquake across the surrounding grid cells in proportion to their distance from the earthquake epicenter. The Gaussian kernel function used in this study is defined in Equation (4).

$$\bar{n}_i = \frac{\sum_j n_j e^{-\frac{d_{ij}^2}{c^2}}}{\sum_j e^{-\frac{d_{ij}^2}{c^2}}} \quad (4)$$

When  $\bar{n}_i$  is the smoothing value,  $n_j$  is the number of earthquakes in cell  $j$ ,  $d_{ij}$  is the distance between cells  $i$  and  $j$ , and  $C$  is the smoothing parameter that controls the extent to which the surrounding area influences a given location. This parameter represents the smoothing distance, which is the spatial boundary within which the value at a given point is still influenced by the values in its vicinity.

The spatial smoothing performed yields a seismic hazard estimation model comparable to the earthquake source zone-based approach. However, this method is more flexible because it does not require the determination or assumption of earthquake source zone boundaries. The performance evaluation of the seismicity smoothing model in this study was conducted using the Molchan diagram [23]. This diagram works by comparing two parameters: the miss rate ( $\nu$ ), which indicates the proportion of earthquakes that the model fails to detect, and the alarm area fraction ( $\tau$ ), which indicates the extent of the area designated as a hazard zone by the model.

The Area Skill Score (ASS) represents an evaluation framework designed to assess the predictive performance of alarm-based earthquake forecasting models, as introduced by [24]. This approach quantifies the degree to which a given prediction model outperforms a predefined reference model, thereby providing a standardized basis for model comparison. The ASS is fundamentally grounded in the concept of the Molchan Diagram, a graphical representation that plots the miss rate ( $\nu$ ) against the fraction of space-time volume occupied by declared alarms ( $\tau$ ) [24]. Within this framework [23], established specific boundary conditions governing the relationship between alarm declarations and event detection: when no alarm is issued, all earthquake events are necessarily missed, whereas when an alarm is declared across the entire testing region, no events remain undetected.

The ASS yields a numerical value spanning from 0 to 1, in which a value of 1 signifies that the forecasting model demonstrates perfect predictive capability, a value of 0 reflects a complete absence of predictive skill, and a value of 0.5 represents the expected outcome for an alarm function that operates entirely at random [24]. Hypothesis testing within the ASS framework is conducted by establishing a null hypothesis that the model performs no better than a random prediction, against an alternative hypothesis indicating the model possesses statistically significant predictive skill [25]. For

this study, Molchan Diagram analysis across multiple bandwidth options yielded an optimal R-score of 0.656 at 100 km bandwidth.

The determination of the attenuation function and the estimation of PGA were carried out using a logic tree framework within the Probabilistic Seismic Hazard Analysis (PSHA) methodology. The theoretical foundation of this estimation is grounded in the total probability theorem, which mathematically integrates contributions from all possible combinations of earthquake magnitude and source-to-site distance to compute the mean annual rate of exceedance of a given ground motion level. The PSHA equations governing this computation are expressed in Equations (5).

$$P[I \geq i] = \iint P[I \geq i | m \text{ and } r] \cdot f_M(m) \cdot f_R(r) \, dm \, dr \quad (5)$$

In the equation above,  $P[I \geq i]$  represents the total probability that the ground motion intensity measure  $I$  exceeds a specified value  $i$  at a given site. The term  $P[I \geq i | m \text{ and } r]$  denotes the conditional probability that the ground motion parameter exceeds a reference value given a specific magnitude  $m$  and distance  $r$ , which is typically derived from Ground Motion Prediction Equations (GMPEs). The functions  $f_M(m)$  and  $f_R(r)$  represent the probability density functions of earthquake magnitude and hypocentral distance, respectively, describing the statistical distribution of seismic sources in the study region [26].

In practice, the input parameters of PSHA cannot be determined with complete certainty due to limited historical earthquake records and incomplete knowledge of active fault systems. This limitation introduces two distinct types of uncertainty: aleatory uncertainty, representing the irreducible natural randomness of the earthquake process embedded within the hazard integral through the probability terms  $P[I \geq i | m \text{ and } r]$ ,  $f_M(m)$ , and  $f_R(r)$  and epistemic uncertainty, arising from incomplete scientific knowledge regarding which model best represents the true physical system [27]. It is for this reason that the logic tree framework becomes necessary in PSHA.

The logic tree provides a systematic procedure in which each node represents a source of epistemic uncertainty such as the choice of seismic source model, recurrence parameters,  $M_{max}$  estimates, or GMPE selection and each branch represents a distinct alternative model assigned a weight reflecting the analyst's degree of belief, with all weights at each node summing to unity. Each complete path through the logic tree yields one fully specified set of input parameters, producing a distinct hazard curve, and the final result is expressed as a weighted distribution of hazard curves from which a weighted mean hazard curve is derived to represent both the central hazard estimate and the range of epistemic uncertainty [28].

In the implementation of this study, three Ground Motion Prediction Equations (GMPEs) were assigned for the active shallow crustal tectonic region to accommodate epistemic uncertainty in ground motion estimation [29], consistent with the depth filter applied in this study (depth < 50.1 km). The selected GMPEs were: the Boore-Atkinson NGA-West2 Ground Motion Model applicable to active shallow crustal earthquakes (M 3.3–8.0) with incorporation of  $V_{s30}$ -dependent site effects [30]. Campbell and Bozorgnia (2014), representing the Campbell-Bozorgnia NGA-West2 Model suitable for shallow crustal earthquakes (M 3.3–7.9) with incorporation of basin depth effects and hanging-wall geometry [31] and Chiou and Youngs (2014), representing the Chiou-Youngs NGA-West2 Model developed with enhanced treatment of nonlinear soil response and depth-to-basement effects [31], applicable to shallow crustal earthquakes (M 3.3–8.5) [32]. Each GMPE was assigned an equal weight of 0.33–0.34 to ensure that the total weight at this logic tree node sums to unity, thereby systematically representing epistemic uncertainty in ground motion characterization. These selections follow the NGA-West2 GMPE framework adopted in Indonesia's national seismic hazard assessment [29], ensuring consistency with the tectonic characteristics of the Indonesian region. The workflow for the Probabilistic Seismic Hazard Analysis (PSHA), including the logic tree nodes for source characterization and ground motion estimation, is presented in Figure 1.

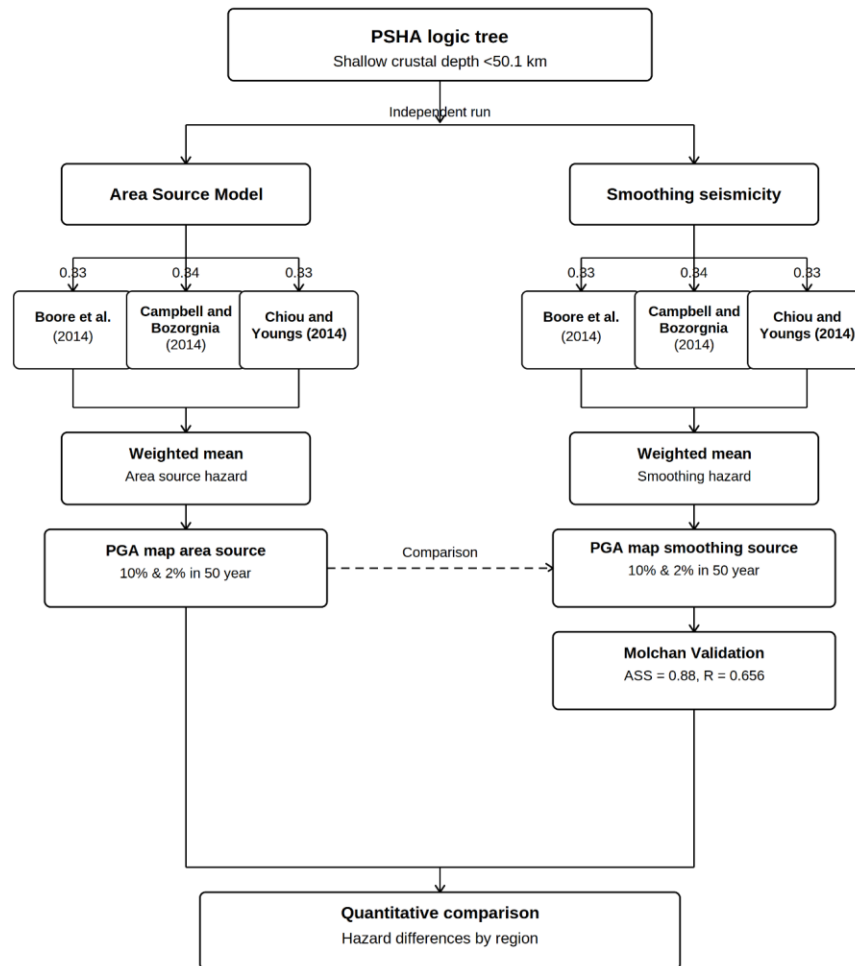


**Figure 1.** Logic tree diagram for seismic hazard modeling using the area source approach, smoothed seismicity, and GMPE weighting.

For the Area Source Model logic tree, the structure comprises two hierarchical levels. At Level 1, the node contains the area source model consisting of 21 tectonic source zones, each characterized by zone-specific Gutenberg-Richter parameters ( $a$ -value and  $b$ -value) derived independently from the earthquake catalog for each zone, with a uniform minimum magnitude ( $M_{min}$ ) of 4.7 and maximum magnitude ( $M_{max}$ ) of 6.5 applied across all zones. The magnitude of completeness ( $M_c$ ) of 4.7 serves as the lower bound for catalog analysis in each zone. At Level 2, three GMPEs are assigned specifically for the active shallow crustal tectonic region. The Area Source Model logic tree produces 1 source model configuration  $\times$  3 GMPEs = 3 complete realizations when fully enumerated. Each complete path through this logic tree yields one fully specified set of input parameters from the area source approach, producing a distinct hazard curve for the area source method.

For the Smoothed Seismicity Model logic tree, the structure also comprises two hierarchical levels, but with different source model characteristics. At Level 1, the node contains the Smoothed Seismicity Model, which employs Gaussian kernel smoothing applied to the declustered ISC catalog spanning 1900–2025. Four bandwidth values were evaluated 25 km, 50 km, 75 km, and 100 km to determine the optimal spatial smoothing parameter. Each bandwidth was assessed using the Molchan Diagram, which measures the spatial forecasting skill of each smoothing result against the observed

seismicity. Based on this evaluation, a bandwidth of 100 km was selected as it demonstrated the best predictive performance with an R-score of 0.656, outperforming the alternative bandwidth values. The selected model is characterized by a Magnitude of Completeness ( $M_c$ ) of 4.4, a minimum magnitude ( $M_{min}$ ) of 4.4, and a maximum magnitude ( $M_{max}$ ) of 6.5, with the 100 km bandwidth applied as the final smoothing parameter.

At Level 2, the same three GMPEs used in the Area Source Model are assigned for the active shallow crustal tectonic region, with identical specifications and equal weighting of 0.33 per GMPE. Equal weighting of 0.33 was assigned to each GMPE to reflect the absence of sufficient regional ground motion data to justify preferring one model over another, and to ensure that epistemic uncertainty in ground motion prediction is represented evenly across the three models, consistent with standard practice in logic tree-based PSHA where no single GMPE can be considered definitively superior [33]. The Smoothed Seismicity Model logic tree produces 1 source model configuration  $\times$  3 GMPEs = 3 complete realizations when fully enumerated. Each complete path through this logic tree yields one fully specified set of input parameters from the smoothed seismicity approach, producing a distinct hazard curve for the smoothed seismicity method.

The two logic trees were executed independently using the same GMPE framework and tectonic region classification, differing only in source characterization: the area source model uses subjectively-delineated zone boundaries, while the smoothed seismicity model employs an objective, data-driven spatial distribution without explicit zone boundaries. This independent execution isolates the effect of source model choice on final PGA estimates and enables direct quantitative comparison between the two approaches under identical GMPE assumptions.

All PSHA calculations were performed using the OpenQuake Engine [34] developed by the Global Earthquake Model (GEM) Foundation, employing the classical PSHA calculator with the following configuration: site mesh spacing of 20, investigation time of 50 years, truncation level of  $3.0\sigma$ , and maximum source-to-site distance of 200 km. The logic tree was fully enumerated to ensure all hazard realizations were computed without Monte Carlo approximation. Hazard outputs include hazard curves and hazard maps computed at two standard probability levels: 10% probability of exceedance in 50 years (return period 475 years) for ordinary building design, and 2% probability of exceedance in 50 years (return period 2,475 years) for critical structure assessment.

### 3. Results and Discussion

The earthquake catalog, after declustering using the Reasenberg method, yielded a Magnitude of Completeness ( $M_c$ ) of 4.7, confirming adequate catalog completeness for PSHA. The Gutenberg-Richter analysis produced a b-value of 0.89 and an a-value of 8.753. The b-value below 1.0 indicates predominance of moderate-to-large magnitude events, characteristic of tectonically complex environments such as subduction zones and strike-slip fault systems. The high a-value reflects elevated overall seismicity consistent with Indonesia's position at the convergence of four major tectonic plates.

Based on the area source model, PGA values under the 10% probability of exceedance in 50 years scenario are presented in Figure 2. PGA values range from 0.04 g to 1.16 g across Indonesia. The highest PGA of 1.16 g was recorded in North Sulawesi (Zone 16), driven by the convergence of the Pacific, Maluku Sea, and Eurasian plates, involving major structures such as the North Sulawesi Trench, the Sangihe Subduction Zone, and active strike-slip faults including the Gorontalo, Palu-Koro, and Matano faults. High PGA values are also concentrated along active subduction zones and fault corridors in Sumatra (1.06 g), Java (1.06 g), Papua (1.02 g), and Bali-Nusa Tenggara (0.85 g). The lowest PGA among Indonesia's major islands was recorded in Kalimantan at 0.04 g, reflecting its stable intraplate position far from active plate boundaries, which is consistent with the finding of Khalqillah, who confirmed that Kalimantan exhibits the lowest seismic hazard compared to other regions in Indonesia, owing to its stable intraplate tectonic setting [35].

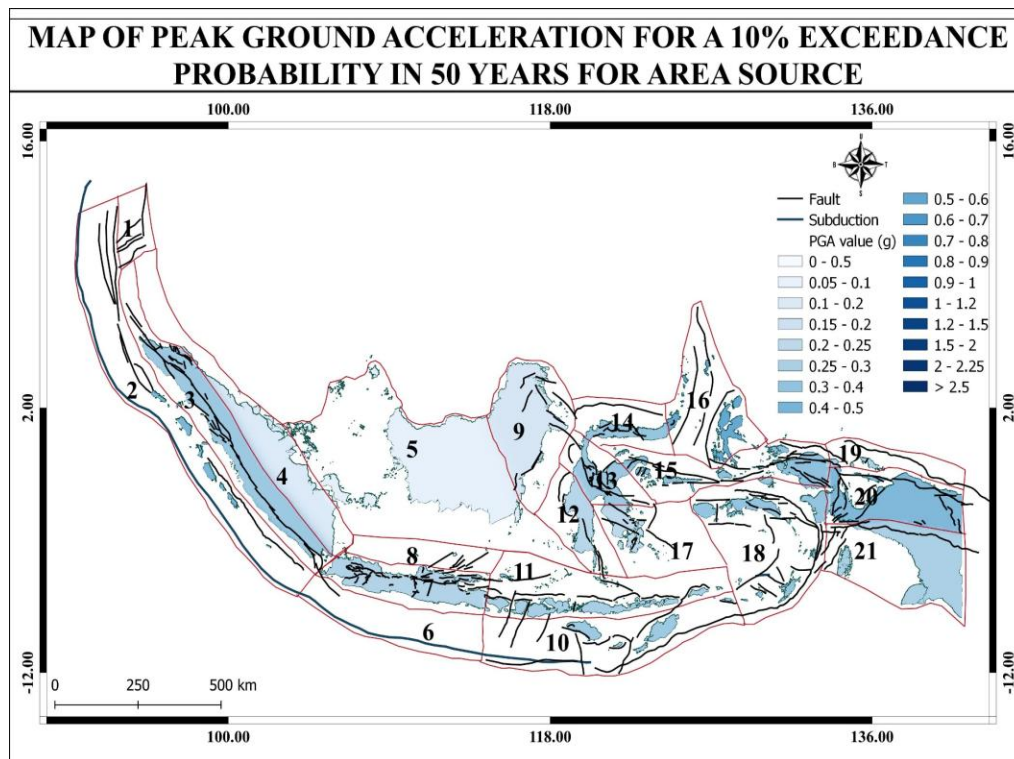


**Figure 2.** PGA Map for a 10% Exceedance Probability Over 50 Years (~475 years) Based on the Area Source Model

Under the 2% probability of exceedance in 50 years scenario shown in Figure 3, PGA values from the area source model range from 0.098 g to 1.59 g, consistently higher than the 10% scenario given the longer return period of 2,475 years. North Sulawesi again recorded the highest value at 1.59 g, followed by Java (1.47 g), Sumatra (1.47 g), and Papua (1.43g). Kalimantan recorded the lowest PGA among major islands at 0.10 g, reflecting its stable tectonic position. The increase in Kalimantan's minimum PGA from 0.04 g in the 10% scenario to 0.10 g in the 2% scenario reflects the contribution of distant large-magnitude sources at very long return periods; even stable intraplate regions exhibit increased seismic hazard when return periods extend to 2,475 years. A key limitation of the area source model is its assumption of spatially uniform seismicity within each predefined zone, which may underestimate localized peak hazard in areas where seismicity concentrates along narrow fault structures, as noted by [36] in the context of national-scale PSHA.

In a previous study conducted by Wulandari [5], the PGA values obtained in the Sumatra region, particularly near the Sumatran Fault, ranged from 1.0 g to 2.0 g. In the present study, one of the observation points located close to the Sumatran Fault yielded a PGA value of 1.06 g. Although both studies employed different seismic source types, different GMPEs, and different input parameters, the resulting PGA value from the present study still falls within the range reported by Wulandari. This similarity can be attributed to the dominant influence of the Sumatran Fault as the primary seismic source in the region and the similar tectonic setting of the study area, which consistently produces significant ground motion energy at the surface regardless of the methodological differences between the two studies.

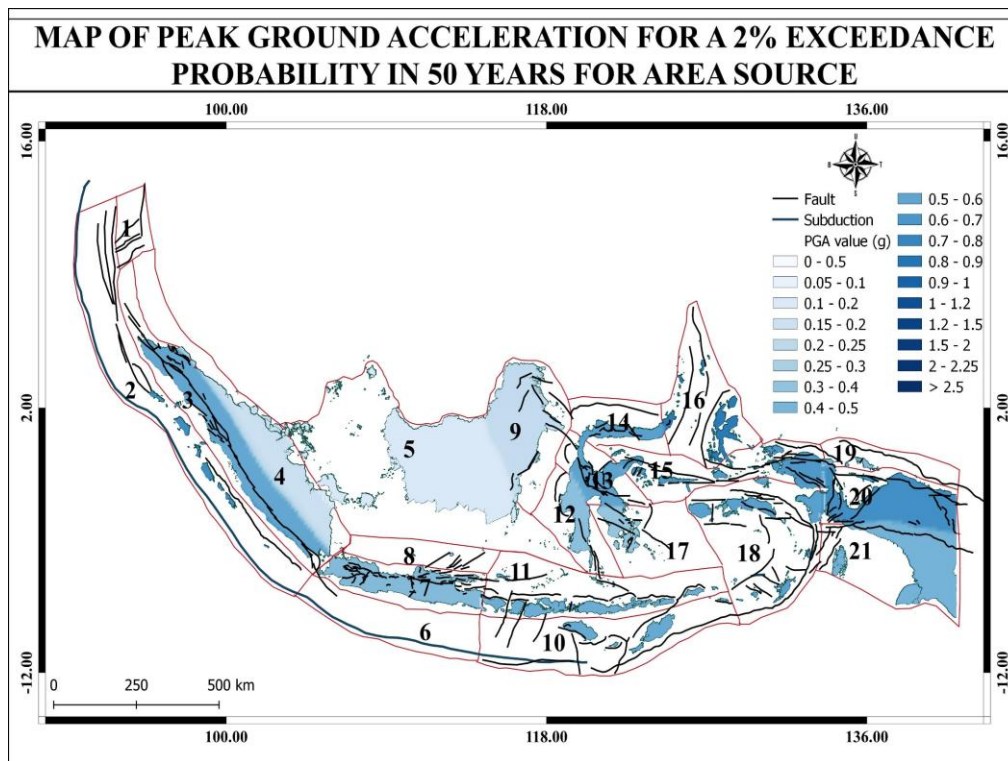


**Figure 3.** PGA Map for a 2% Exceedance Probability Over 50 Years (~2475 years) Based on the Area Source Model

For this study, the bandwidth (C) was set to 100 km, selected based on validation through the Molchan Diagram analysis. The earthquake catalog was divided into two subsets: a training dataset covering 1900–2015, used to construct the seismicity model and estimate spatial smoothing rates, and a testing dataset covering 2016–2025, used to evaluate the model's predictive performance. Four bandwidth values were evaluated 25 km, 50 km, 75 km, and 100 km and the 100 km bandwidth demonstrated optimal forecasting skill (R-score = 0.656) as shown in Figure 4. The Area Skill Score (ASS) of 0.88 substantially exceeds the random forecast threshold of 0.5 and approaches the theoretically perfect score of 1.0, confirming that the smoothed seismicity model is both statistically significant and skillful in capturing the spatial distribution of seismicity within Indonesia. The results indicate that the smoothing-based seismicity model constructed from historical data successfully confirms the tendency of future earthquakes to occur in spatial proximity to past seismic activity, consistent with the fundamental assumption of the seismicity smoothing method [7].

These validation results are comparable to those reported by Danciu [37] for the ESHM20, where kernel-based smoothing models with adaptive bandwidth achieved high spatial forecasting skill across diverse tectonic environments, and are consistent with the validation framework applied by Rahman [36] for Pakistan, where smoothed seismicity models were evaluated against independent earthquake catalogs. The absence of an equivalent Molchan validation for the area source model in this study represents a limitation that future work should address to enable direct performance comparison between the two approaches.

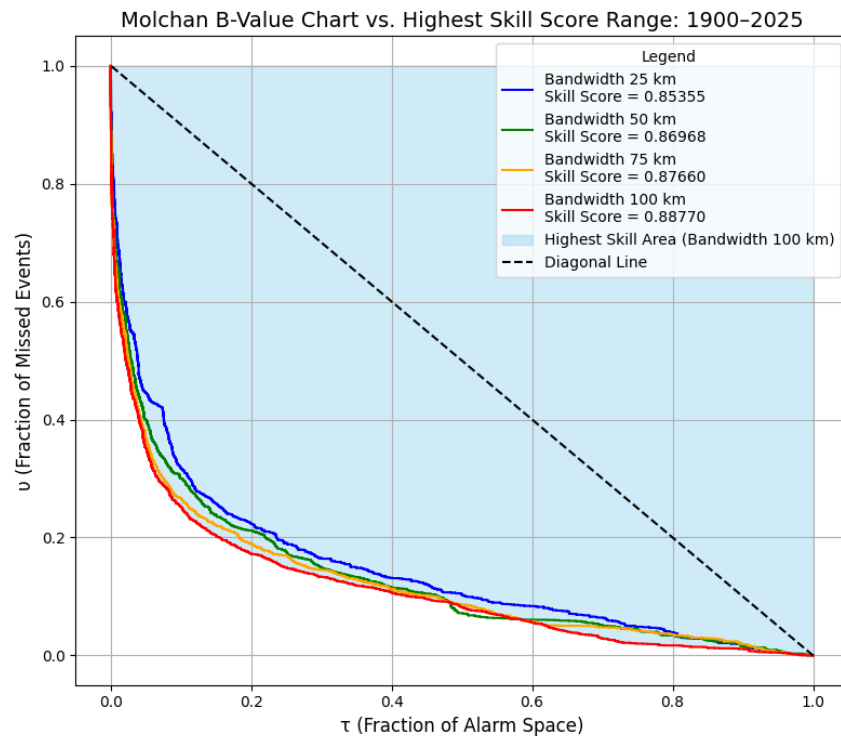


**Figure 4.** Molchan Diagram

The smoothed seismicity model results for the 10% probability of exceedance in 50 years scenario are presented in Figure 5. PGA values range from 0.00 g to 2.13 g, with the maximum consistently located in North Sulawesi. The near-zero minimum PGA values in certain grid cells are a direct mechanical consequence of the kernel-based approach, arising from three conditions: the absence of recorded earthquakes within the effective kernel radius, the exclusion of earthquakes below the completeness magnitude ( $M_c$ ), and the distance of a region from the center of historical seismic activity, which causes the spatial smoothing kernel to assign minimal weight to areas with no nearby recorded seismicity. These conditions collectively explain why certain grid cells yield zero or near-zero seismicity smoothing values, a behavior fundamentally different from the area source model, which assigns a background seismicity rate to all zones regardless of historical earthquake density, thereby preventing zero-value gaps. This behavior is consistent with the findings of Danciu [37] for the European Seismic Hazard Model, where adaptive kernel smoothing similarly produced near-zero hazard in regions with sparse historical seismicity.

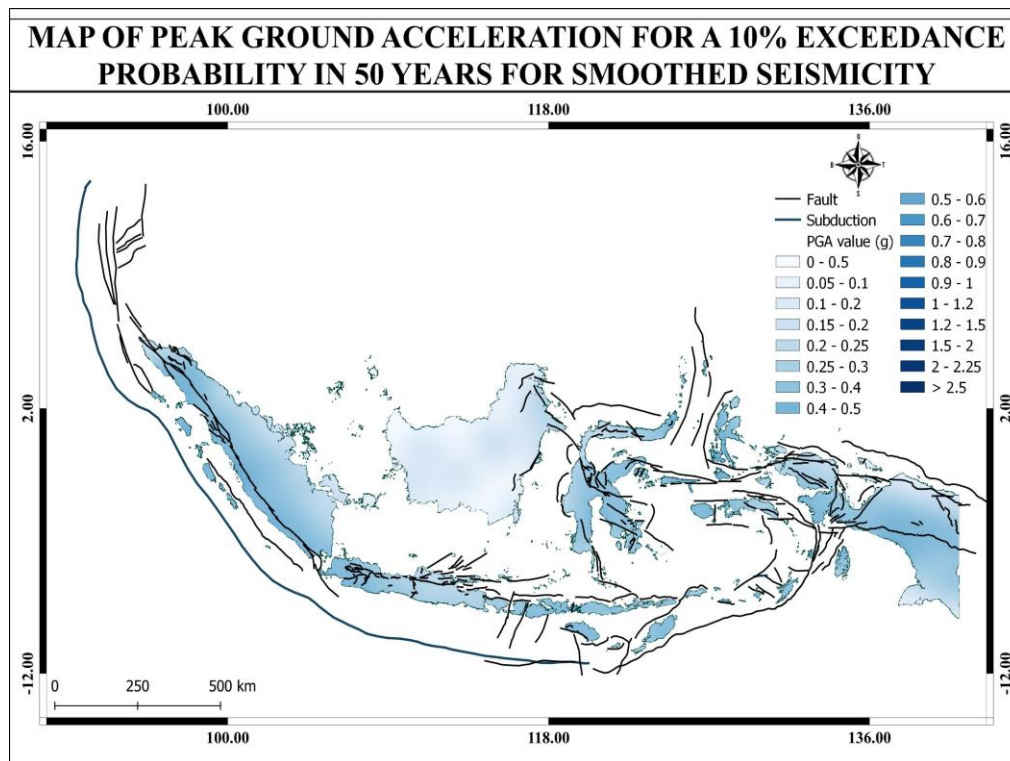


**Figure 5.** PGA map for a 10% exceedance probability in 50 years (~475 years) based on seismicity smoothing.

Under the 2% probability of exceedance in 50 years scenario shown in Figure 6, the smoothed seismicity model maintains the same maximum PGA of 2.13 g in North Sulawesi, while minimum values range from 0.00 g to 0.05 g in the interior of Kalimantan and deep ocean areas. The spatial pattern remains consistent with the 10% scenario, but with intensities reflecting less frequent and larger earthquakes.

The smoothed seismicity model yielded substantially higher maximum PGA values than the area source model in both scenarios: 2.13 g versus 1.5901 g in the 2% scenario, and 2.13 g versus 1.1597 g in the 10% scenario. This discrepancy is physically explained by the ability of the smoothed model to concentrate seismicity rates at historically active grid cells without spatial averaging across broad zones. In the area source approach, seismicity is distributed uniformly across each zone, effectively diluting localized concentrations of historical earthquakes. The smoothed approach preserves these spatial gradients, producing sharper hazard peaks in tectonically complex regions. This finding is consistent with [36], who demonstrated that smoothed seismicity models produce higher localized hazard estimates in regions of concentrated historical seismicity compared to uniform zone models, and with [37], who showed that kernel-based models capture spatial heterogeneity more effectively than zone-based models in seismically diverse environments. The sensitivity of the smoothed model to kernel bandwidth selection represents an important source of uncertainty. The 100 km bandwidth adopted in this study reflects a compromise between spatial resolution and catalog density, consistent with the regional-scale approach recommended by [38] and applied in national-scale hazard assessments such as [39] for the United States.

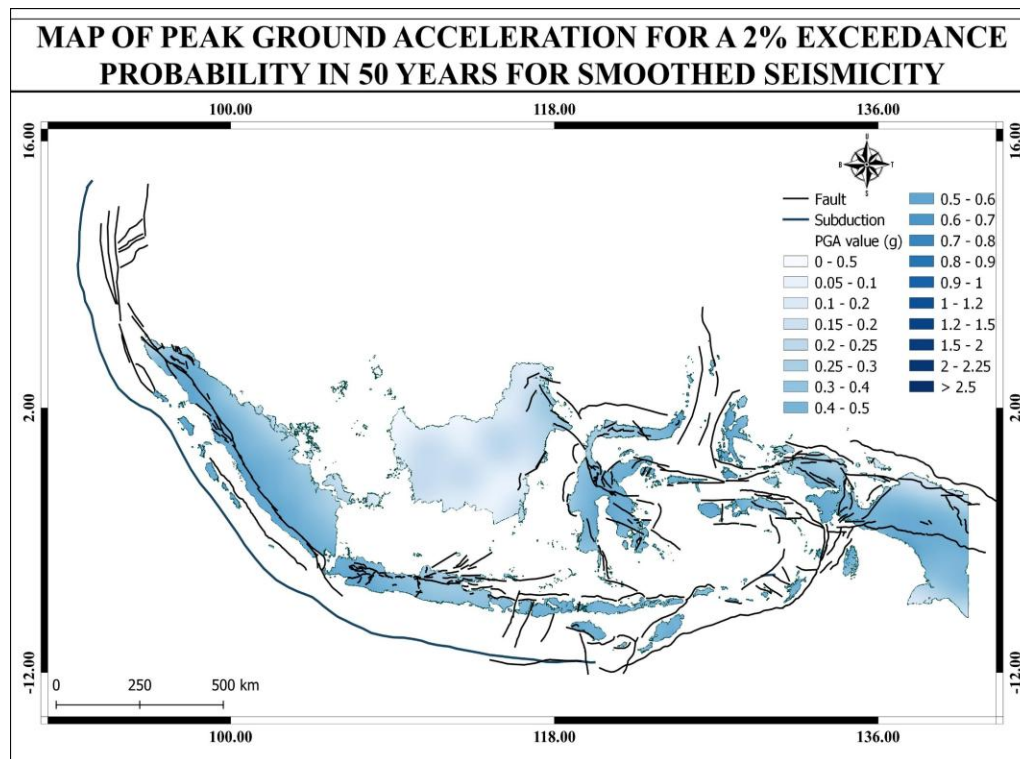


**Figure 6.** PGA map for a 2% exceedance probability in 50 years (~2475 years) based on seismicity smoothing.

Furthermore, Wulandari [11] also conducted a study comparing area source and smoothed seismicity approaches in the Sumatra region, in which both methods were employed as complementary approaches. The area source model was used to capture broad seismic trends within defined geographic regions, while the smoothed seismicity model applied varying bandwidths to highlight seismic hazard patterns across space. For model validation, Wulandari utilized the Molchan Diagram as a critical tool to assess the predictive accuracy of both the area source and smoothed seismicity models. Similarly, the present study also applies both area source and smoothed seismicity approaches, with shallow crustal earthquakes as the common seismic source used in both studies. However, a limitation exists in the present study, as model validation using the Molchan Diagram was only performed for the smoothed seismicity model, while the area source model was not subjected to the same validation procedure.

A systematic comparison between the two models reveals both consistent spatial patterns and important quantitative differences. Both models agree that North Sulawesi represents the highest seismic hazard region and Kalimantan the lowest among Indonesia's major islands, reflecting the well-established tectonic framework of the Indonesian archipelago. The smoothed model better captures spatial heterogeneity where the catalog is dense and complete, while the area source model provides more stable estimates in regions with sparse seismic data. The independent results from both models demonstrate that they produce complementary spatial information, suggesting that future PSHA implementations in Indonesia could benefit from integrating both approaches within a logic tree framework, as demonstrated by [36] for Pakistan and [37] for Europe, where equal weighting between the two source models reduced epistemic uncertainty in national-scale hazard estimates.

#### 4. Conclusion

This study compared area source and smoothed seismicity approaches for PSHA across Indonesia, revealing both consistent spatial patterns and significant quantitative differences. Both models consistently identified North Sulawesi as the highest hazard region and Kalimantan as the lowest, reflecting Indonesia's complex tectonic framework. However, the smoothed seismicity model produced higher maximum PGA values than the area source model in both scenarios: 2.13 g versus 1.1597 g at 10% probability of exceedance in 50 years, and 2.13 g versus 1.5901 g at 2% probability of exceedance in 50 years, because the smoothed model preserves localized seismicity concentrations whereas the area source model dilutes them through uniform zone averaging.

Validation using the Molchan Diagram yielded an Area Skill Score of 0.88 and an R-score of 0.656, confirming strong spatial forecasting skill of the smoothed seismicity model well above the random forecast threshold of 0.5. The two approaches are complementary: the smoothed model captures spatial heterogeneity in catalog-dense regions, while the area source model provides stable estimates where historical seismicity data are sparse. Future national-scale PSHA in Indonesia would benefit from integrating both methods within a logic tree framework to produce more robust seismic hazard estimates for earthquake risk mitigation and building code development.

#### References

- [1] S. Dey Rahmawati. (2025). Spatial Modeling of Earthquake Risk in Sulawesi and Maluku Based on Geological Factors, *ESTIMASI: Journal of Statistics and Its Application*, vol. 6, no. 2, pp. 2721–379.
- [2] N. R. Ananda and D. Pujiastuti. (2024). Studi Bahaya Seismik dengan Metode PSHA (Probabilistic Seismic Hazard Analysis) di Nusa Tenggara Barat Menggunakan Data Gempa Tahun 1900 - 2023, *Jurnal Fisika Unand*, vol. 13, no. 5, pp. 665–670.
- [3] M. M. Gallahue et al. (2022). A study on the effect of site response on California seismic hazard map assessment, *Front. Earth Sci. (Lausanne)*, vol. 10.
- [4] R. I. Hielmy and M. L. Rajagukguk. (2026). Analisis Probabilistik Bahaya Seismik Di Denpasar Dan Sekitarnya Berdasarkan Pendekatan Psha, *KURVATEK*, vol. 11, no. 1, pp. 21–28.
- [5] R. Wulandari, C.-H. Chan, J.-C. Gao, and D. H. Natawidjaja. (2024). Probabilistic Seismic Hazard Assessment of Sumatra, Indonesia, *Research Square*.
- [6] A. Daswita, D. Pujiastuti, T. Anggono, F. Bumi, J. Fisika, and F. Matematika dan Ilmu Pengetahuan Alam. (2023). Studi Bahaya Seismik dengan Metode Probabilistic Seismic Hazard Analysis di Sumatera Barat, *Jurnal Fisika Unand*, vol. 12, no. 3, pp. 445–451.
- [7] A. Frankel. (1995). Mapping Seismic Hazard in the Central and Eastern United States, *Seismological Research Letters*, vol. 66, no. 4, pp. 8–21.
- [8] A. Saputra. (2024). Implementasi Metode Smoothing Seismicity Dalam Analisis Distribusi Gempa Bumi Pada Data Seismisitas (1900-2024) Di Wilayah Indonesia, *Repository ITERA*.
- [9] R. Mountainshia, P. Pramono Rahardjo, and D. Damara Aditramulyadi. (2022). Analisis Probabilitas Bahaya Gempa di Ibu Kota Baru Indonesia, *USGS Report / Online Open Source*.
- [10] M. M. Rahman, L. Bai, H. Li, and C. Liu. (2025). Probabilistic Seismic Hazard Map for Bangladesh Including the Smoothed Background Seismicity and Local Site Effects, *Pure and Applied Geophysics*.
- [11] R. Wulandari and Y. Styawan. (2026). Enhancing Seismic Hazard Preparation in Lampung, Sumatra: Improved Magnitude Conversion, Seismicity Smoothing, and Area-Source Modeling, *Indonesian Journal on Geoscience*, vol. 13, no. 2, pp. 189–209.
- [12] C. H. Chan et al. (2020). Probabilistic seismic hazard assessment for Taiwan: TEM PSHA2020, *Earthquake Spectra*, vol. 36, no. 1\_suppl, pp. 137–159.
- [13] T. C. Hanks and H. Kanamori. (1979). A moment magnitude scale, *Journal of Geophysical Research: Solid Earth*, vol. 84, no. B5, pp. 2348–2350.

- 
- [14] P. Reasenbergl. (1985). Second-order moment of central California seismicity, 1969–1982, *Journal of Geophysical Research: Solid Earth*, vol. 90, no. B7, pp. 5479–5495.
- [15] R. Hanafi, I. Kusuma Dewi, and N. Ngatijo. (2024). Pemetaan Magnitude Of Completeness (Mc) Untuk Gempa Di Wilayah Bengkulu, *JGE (Jurnal Geofisika Eksplorasi)*, vol. 10, no. 2, pp. 121–138.
- [16] M. Irsyam et al. (2020). Development of the 2017 national seismic hazard maps of Indonesia, *Earthquake Spectra*, vol. 36, no. 1\_suppl, pp. 112–136.
- [17] R. Lewerissa, R. Rumakey, Y. A. Syakur, and L. Lapono. (2021). Completeness magnitude (Mc) and b-value characteristics as important parameters for future seismic hazard assessment in the West Papua province Indonesia, *Arabian Journal of Geosciences*, vol. 14, no. 23, p. 2588.
- [18] V. A. Ritz, A. P. Rinaldi, and S. Wiemer. (2022). Transient evolution of the relative size distribution of earthquakes as a risk indicator for induced seismicity, *Communications Earth & Environment*, vol. 3, no. 1, p. 249.
- [19] G. M. Geffers, I. G. Main, and M. Naylor. (2023). Accuracy and precision of frequency-size distribution scaling parameters as a function of dynamic range of observations: example of the Gutenberg-Richter law b-value for earthquakes, *Geophysical Journal International*, vol. 232, no. 3, pp. 2080–2086.
- [20] A. Kijko and A. Smit. (2017). Estimation of the frequency-magnitude Gutenberg-Richter B-value without making assumptions on levels of completeness, *Seismological Research Letters*, vol. 88, no. 2A, pp. 311–318.
- [21] M. Taroni and A. Akinci. (2021). A new smoothed seismicity approach to include aftershocks and foreshocks in spatial earthquake forecasting: Application to the global  $m_w \geq 5.5$  seismicity, *Applied Sciences*, vol. 11, no. 22, p. 10899.
- [22] J. K. Lapajne, B. Šket Motnikar, B. Zabukovec, and P. Zupančič. (1997). Spatially smoothed seismicity modelling of seismic hazard in Slovenia, *Journal of Seismology*, vol. 1, no. 1, pp. 73–85.
- [23] G. Molchan and V. Keilis-Borok. (2008). Earthquake Prediction: Probabilistic Aspect, *Geophysical Journal International*, vol. 173, no. 3, pp. 1012–1017.
- [24] J. D. Zechar and T. H. Jordan. (2008). Testing alarm-based earthquake predictions, *Geophysical Journal International*, vol. 172, no. 2, pp. 715–724.
- [25] E. Biondini, F. D’Orazio, B. Lolli, and P. Gasperini. (2025). Pseudo-prospective earthquake forecasting experiment in Italy based on temporal variation of the b-value of the Gutenberg–Richter law, *Geophysical Journal International*, vol. 240, no. 3, pp. 1755–1772.
- [26] C. A. Cornell. (1968). Engineering Seismic Risk Analysis, *Bulletin of the Seismological Society of America*, vol. 58, no. 5, pp. 1583–1606.
- [27] M. P. Moschetti et al. (2024). The 2023 US National Seismic Hazard Model: Ground-motion characterization for the conterminous United States, *Earthquake Spectra*, vol. 40, no. 2, pp. 1158–1190.
- [28] G. Kaviris et al. (2023). A Logic-Tree Approach for Probabilistic Seismic Hazard Assessment in the Administrative Region of Attica (Greece), *Applied Sciences*, vol. 13, no. 13, p. 7553.
- [29] D. M. Boore, J. P. Stewart, E. Seyhan, and G. M. Atkinson. (2014). NGA-West2 equations for predicting PGA, PGV, and 5% damped PSA for shallow crustal earthquakes, *Earthquake Spectra*, vol. 30, no. 3, pp. 1057–1085.
- [30] K. W. Campbell and Y. Bozorgnia. (2014). NGA-West2 ground motion model for the average horizontal components of PGA, PGV, and 5% damped linear acceleration response spectra, *Earthquake Spectra*, vol. 30, no. 3, pp. 1087–1115.
-

- 
- [31] B. S. J. Chiou and R. R. Youngs. (2014). Update of the Chiou and Youngs NGA model for the average horizontal component of peak ground motion and response spectra, *Earthquake Spectra*, vol. 30, no. 3, pp. 1117–1153.
- [32] Pusat Studi Gempa Nasional (Indonesia). (2017). Peta sumber dan bahaya gempa Indonesia tahun 2017, *Pusat Penelitian dan Pengembangan Perumahan dan Permukiman, Kementerian Pekerjaan Umum*.
- [33] F. Scherbaum and N. M. Kuehn. (2011). Logic tree branch weights and probabilities: Summing up to one is not enough, *Earthquake Engineering Research Institute*.
- [34] GEM Foundation. (2019). The OpenQuake-engine User Manual, *Global Earthquake Model (GEM) OpenQuake Manual for Engine version 3.5.0*.
- [35] A. Khalqillah, M. Umar, A. V. H. Simanjuntak, A. Jihad, and V. H. Banyunegoro. (2025). Seismic Hazard Estimation for Sumatra and Kalimantan Region Using Event-Based Probabilistic Seismic Hazard Analysis (EB-PSHA), *Journal of Geoscience, Engineering, Environment, and Technology*, vol. 10, no. 3, pp. 329–337.
- [36] A. ur Rahman, F. A. Najam, S. Zaman, A. Rasheed, and I. A. Rana. (2021). An updated probabilistic seismic hazard assessment (PSHA) for Pakistan, *Bulletin of Earthquake Engineering*, vol. 19, no. 4, pp. 1625–1662.
- [37] L. Danciu et al. (2024). The 2020 European Seismic Hazard Model: overview and results, *Natural Hazards and Earth System Sciences*, vol. 24, no. 9, pp. 3049–3073.
- [38] G. Woo. (1996). Kernel Estimation Methods for Seismic Hazard Area Source Modeling, *Bulletin of the Seismological Society of America*, vol. 86, no. 2, pp. 353–362.
- [39] M. D. Petersen et al. (2024). The 2023 US 50-State National Seismic Hazard Model: Overview and implications, *Earthquake Spectra*, vol. 40, no. 1, pp. 5–88.